Active thermal management for a single-phase H-Bridge inverter employing switching frequency control

Markus Andresen
Giampaolo Buticchi
Johannes Falck
Marco Liserre
Ole Muehlfeld

Suggested Citation

Active thermal management for a single-phase H-Bridge inverter employing switching frequency control

Markus Andresen, Giampaolo Buticchi, Johannes Falck, Marco Liserre, Ole Mühlfeld*

Chair of Power Electronics, Christian-Albrechts-Universität zu Kiel, Kaiserstraße 2, Germany

* Danfoss Silicon Power GmbH

ma@tf.uni-kiel.de, gibu@tf.uni-kiel.de, jofa@tf.uni-kiel.de, ml@tf.uni-kiel.de

ole.muehlfeld@danfoss.com

Abstract

A thermal controller can be employed to reduce the thermal swing consequent to power cycling. This is demonstrated in this work for a full bridge inverter without *a priori* knowledge of the mission profile to which the converter is a subsystem, with the objective to reduce the thermal cycling without measurement of the junction temperature. The performance of the thermal controller is experimentally demonstrated by comparing a system, which operates with constant switching frequency with a system equipped with differently tuned thermal controllers. The impact of active thermal control on lifetime is investigated.

1) Introduction

Power electronic converters are widely used for electric vehicles, aircrafts and grid connected applications, such as renewable energies. The reliability of these systems is essential, because failures cause downtimes and thus costs [1]. The most important failure mechanism is based on thermal cycling and is addressed in [2],[3]. Thermal cycling is affected by ambient temperature variations and power cycling, leading to mechanical stress within the module, which causes aging and finally failures. Semiconductor manufacturers optimize hardware to increase the reliability. Beside improved hardware, active thermal control enables to decrease the effects of power cycling [4]. However, in many systems, the main target is to maximize the efficiency, which is especially true in photovoltaic applications. Another way to improve the cost efficiency is to increase the lifetime of the system by a reduction of thermal cycling. In [5]

active thermal control has been introduced to drive the system in safe operation during a fault of a subsystem, but not to increase lifetime during normal operation.

This work proposes to modify the switching frequency to control the semiconductor losses, leading to reduced thermal cycles and increased lifetime under fast changing load conditions. The thermal control relies on electrical measurements and does not require additional sensors to reduce the thermal cycling. It is shown that the appropriate tuning is mandatory to find the optimal system behavior.

The active thermal control is first described in theory and then tested on an experimental setup consisting of an H-bridge inverter connected to a passive load.

2) Active thermal control

The junction temperature T_j of the power semiconductors depends on the losses of the device P_{loss}, the thermal resistance between junction to ambient $R_{th,ja}$ and the ambient temperature T_a.

$$T_j = T_a + P_{loss} \cdot R_{th,ja} \qquad (1)$$

Since the ambient temperature cannot be influenced and the thermal resistance is dependent on the hardware, the losses are controlled to reduce the thermal cycling. In high power applications, usually the switching losses P_{sw} and the conduction losses P_{cond} are dominant, while driving or blocking losses are neglected:

$$P_{loss} = P_{sw} + P_{cond} \qquad (2)$$

The conduction losses can be approximated with a second order polynomial, where i_{load}^{pk} is the peak alternating current, m is the modulation factor and $\cos(\phi)$ is the power factor:

$$P_{cond} = \left(\frac{1}{2\pi} + \frac{m \cdot cos(\phi)}{8}\right) \cdot u_{ce,0} \cdot i_{load}^{pk} + \left(\frac{1}{8} + \frac{m \cdot cos(\phi)}{3\pi}\right) \cdot r_{ce} \left(i_{load}^{pk}\right)^2 \qquad (3)$$

The switching losses can be expressed with the turn on losses E_{on}, the turn off losses E_{off}, the switching frequency f_{sw}, the dc-link voltage U_{dc}, the load current and an empirical factor c, suggested to be chosen to 1.3 in [7]

$$P_{sw} = f_{sw} \cdot \left(E_{on} + E_{off}\right) \cdot \frac{i_{load}^{pk}}{I_{ref}} \left(\frac{U_{dc}}{U_{dc,ref}}\right)^c \qquad (4)$$

Based on the bondwire liftoff failure mechanism, which is characterized by the Coffin-Manson equation, the power semiconductors can undergo an specific number of thermal cycles N_f, which is exponentially dependent on the magnitude of the thermal cycles ΔT_j and average temperature T_j. $A = 302500$, $\alpha = -5.039$ and $E_a = 9.89E - 20$ are the Scheuermann fitting parameters, found for average power modules while k is the Boltzmann constant. As can be seen from the α value, the importance of the amplitude of the thermal for lifetime is critical.

The impact of T_j is less relevant, but an increased temperatures reduces the expected lifetime as well.

$$N_f = A(\Delta T_J)^\alpha e^{\left(\frac{E_a}{kT_J}\right)} \tag{5}$$

The idea proposed in this paper is to reduce the thermal cycling by regulating determined profiles of losses via switching frequency variations. Some hypothesis will be considered: The full-bridge (shown in Figure 1) operates in hard-switching conditions at variable modulation ratio on a RL load. The H-bridge is driven by a unipolar modulation (with freewheeling in the upper and lower sides of the H-bridge). The modulation index is changed according to a mission profile.

Figure 2 shows the proposed control method. The common operation resides in the losses model, shown in equations (3) and (4), that allows estimating the average losses over a fundamental output period. The difference between the actual losses and a low-pass filtered version constitutes the power difference that the active thermal control aims at reducing.

A look-up table that links the power difference to the frequency increase is adopted, so that a higher switching frequency is selected when the output power is reducing (with gain $\frac{\Delta f_{max}}{\Delta P_{max}}$). Instead, when the output power is increasing, the switching frequency is locked to the minimum. This non-linear control aims at preventing the cooling of the power module when the output power is reduced, but does not work when the modules is heating up. This behavior
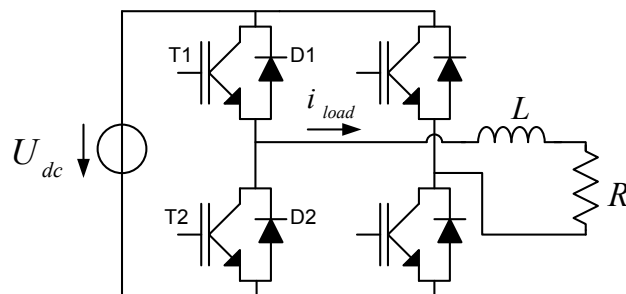

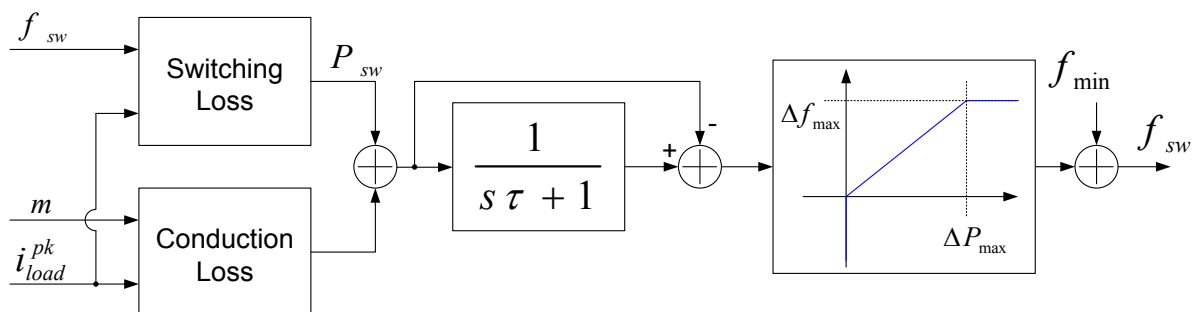Figure 1. Schematic of an H-Bridge connected to a passive load.

Figure 2. Block scheme of the Active Thermal Control.

actually limits the increase of the switching frequency, reducing the additional losses introduced by the active thermal control. The tuning parameters of the control are represented by the gain $\frac{\Delta f_{max}}{\Delta P_{max}}$, that should be tuned to have the maximum allowed frequency in the case of the maximum power difference, and the time constant τ, that selects the speed of the control.

3) Laboratory setup and measurement results

The thermal control algorithm is tested on a full bridge converter module (DP25H1200T101667-101667, $V_{ce} = 1200\ V$, $I_c = 25\ A$) built by Danfoss as shown in figure 3. An RL load is connected to the inverter ($R = 15\ \Omega$, $L = 4.5\ mH$) and the inverter generates a sinusoidal output voltage ($f = 50Hz$). To enable direct chip contact for the junction temperature measurement, there is no gel in the module, which reduces the maximum isolation voltage. The temperature detection is done with an optic fiber measurement system (Opsens Prosens) equipped with sensors, which obtain a response time of *5 ms* to temperature variations. The case temperature is sensed with an NTC.
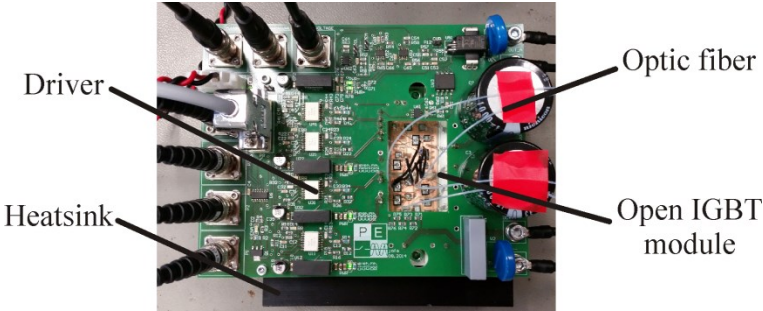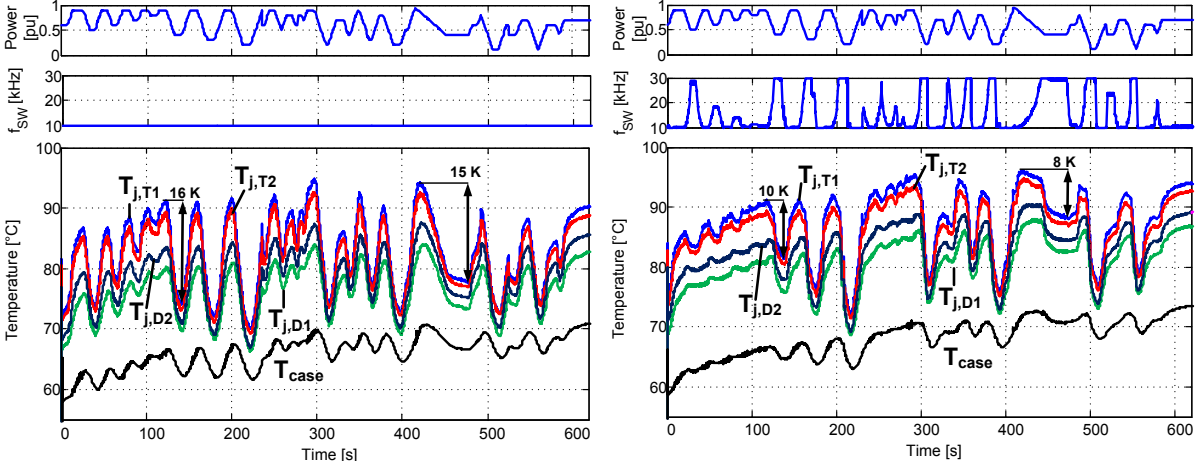

Figure 3. Experimental setup.

(a) Constant switching Frequency.

(b) Active Thermal Control with τ=1s.

Figure 4. Junction temperature measurement for $U_{dc} = 350\ V$ and a variation of the modulation index with and without active thermal control.

For an evaluation of the thermal controller, the minimum switching frequency of the inverter is assumed to be $f_{min} = 10\ kHz$ and the maximum increase $\Delta f_{max} = 20\ kHz$. First, the controller is tested for constant $f_{SW} = f_{min}$, which is assumed to be the standard case for a cost effective system design. Secondly, the thermal controller is tested for different filter constants $\tau = [0.1\ s, 1\ s, 10\ s]$ to evaluate the reduction of thermal cycling. Before the mission profile is started, the converter is heated up until the temperatures reach steady state. In figure 4 a) the junction temperature measurement for the operation with constant switching frequency is shown. The junction temperature of all power semiconductors is correlated to the mission profile and undergoes high thermal cycles. Differences in the temperatures of IGBTs and diodes can be explained with the design of the module. In figure 4 b) the thermal controller is activated for the same mission profile and $\tau = 1s$. The switching frequency increases for a reduction of the modulation index and decreases after time or with an increase of the modulation index. It can be seen from the waveforms that the magnitude of some thermal cycles is decreased. In order to visualize the reduction of thermal cycling, the rainflow counting algorithm is applied. All thermal cycles with a magnitude lower than $\Delta T < 1\ K$ are neglected, because their contribution to the aging is very low.

In figure 5 a) this is shown for the IGBT 1 under constant switching frequency and for the activation of the thermal controller with different filter time constants in figure 5 b)-d). The
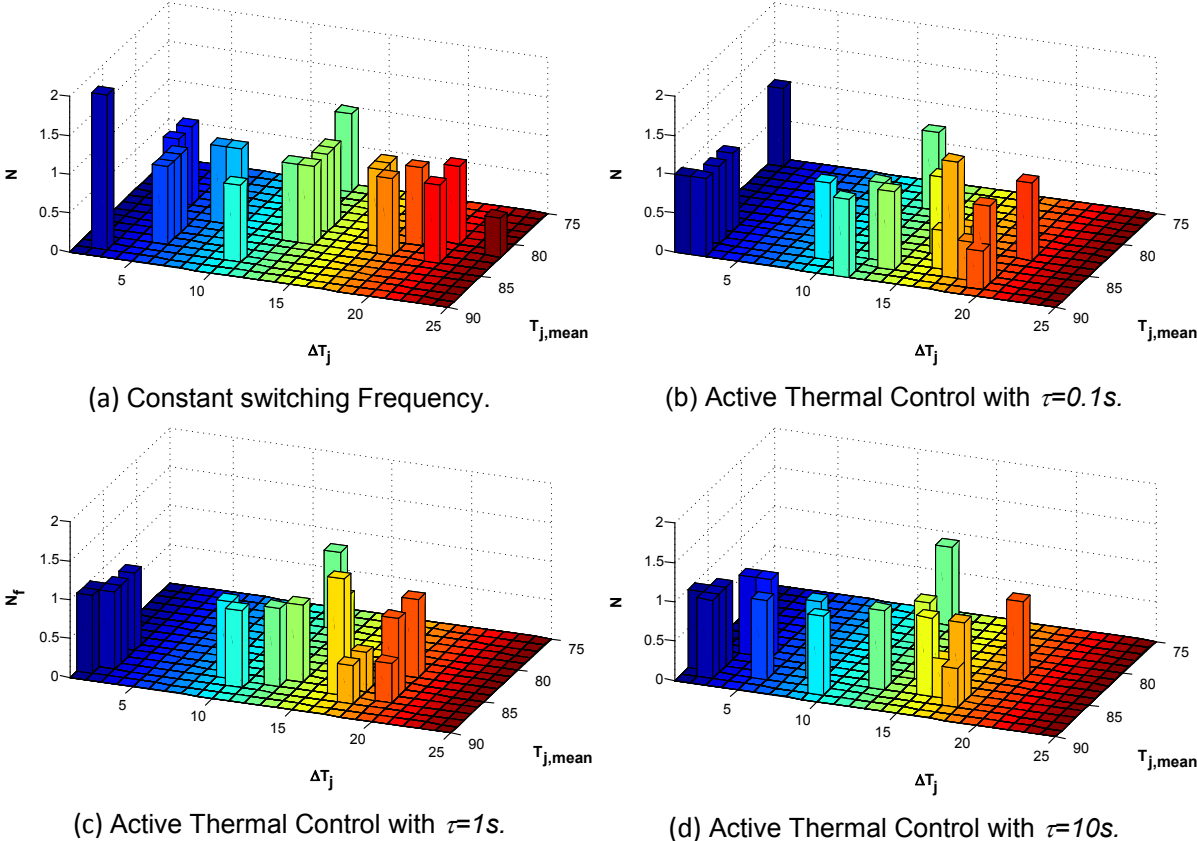

(a) Constant switching Frequency.

(b) Active Thermal Control with τ=0.1s.

(c) Active Thermal Control with τ=1s.

(d) Active Thermal Control with τ=10s.

Figure 5. Measurement results after rainflow counting for IGBT T1.

resolution of the rainflow matrix is set to $1\,K$ for the thermal swing ΔT_j as well as the average temperature $T_{j,mean}$.

For the constant switching frequency, the most severe thermal cycles for the power electronic module are at a magnitude of $\Delta T = 25\,K$ and there are cycles with a magnitude of $\Delta T = 21\,K$. Further thermal cycles with lower magnitude are affected, whereby the average temperature is mostly between $80\,K < T_{j,mean} < 85\,K$. In a comparison to the activated thermal control, the maximum thermal cycles are reduced to a magnitude lower than $\Delta T < 21K$ and also all other high thermal cycles are significantly reduced.

Different time constants for the thermal controller lead to different shape of the histogram. Larger time constants achieve a greater reduction of the high magnitude thermal cycles. The cost for this improvement is a higher average temperature. In table 1 the basic parameters for of the comparison are shown. This is the total average temperature during the whole experiment $T_{j,av}$, the average switching frequency $f_{sw,av}$, the accumulated thermal cycles $\sum \Delta T$ (for $\Delta T > 1K$) and the relative losses energy $E_{loss,rel}$ as normed integral derived from (1). The index x represents a power semiconductor, $T_{j,x,const}$ stands for the temperature measurement of the power semiconductor for a constant switching frequency and T_{ges} stands for the length of the mission profile.

$$E_{loss,rel}(x) = \frac{\int_0^{T_{ges}}(T_{j,x}-T_c)\,dt}{\int_0^{T_{ges}}(T_{j,x,const}-T_c)\,dt} \qquad (6)$$

The thermal control affects an increased switching frequency, which leads to an increased junction temperature and reduced thermal cycles, while also the loss energy is increased between 5.8% and 7.4%. In this case a reduction of the cumulated thermal cycles by approximately $30\,\%$ is achieved, while the average temperature is increased by $5-7\,K$. The comparison between the different filter time constants does not lead to a clear trend for superior behavior. It should be noted, that an increase in the switching frequency improves the power quality and reduces the losses in the filter.

The same analysis can be done for the diodes. Rainflow counting is applied for the diode D1 for the similar experiments as for the IGBT 1. The results for a constant switching frequency are shown in figure 6 a) with a resolution of $1\,K$ for the thermal cycles and $2\,K$ for the average

	No thermal control	Thermal control, $\tau = 0.1s$	Thermal control, $\tau = 1s$	Thermal control, $\tau = 10s$
$T_{j,av}$ [°C]	82,50	89,19	87,80	87,88
$\sum \Delta T$ [K]	265,26	178,64	176,74	181,50
$f_{sw,av}$ [kHz]	10	14,60	15,02	14,90
$E_{loss,rel}$ [%]	100	107,4	105,8	105,9

Table 1. Comparison of the thermal stress in IGBT 1 for different controller settings.

temperature of the cycle. The highest thermal cycle has a magnitude of $\Delta T = 17K$ and lower thermal swings occur for most magnitudes. The average temperature for the thermal cycles is around 76 K. The experiment with active thermal control is shown in figure 6 b)-d). Similar to the IGBT case, all thermal cycles are reduced in magnitude, while the average temperature is increased. Higher filter time constants τ lead to a reduction of the maximum thermal swing. In table 2 the average temperature and the accumulated thermal cycles are shown as well as the relative loss energy of the system. The relative losses are comparable to the relative losses of the IGBT 1 and the accumulated cycles decrease with an increase of τ. However, by also taking into account average temperature, the switching frequency and the efficiency, there is no solution superior in all criteria.
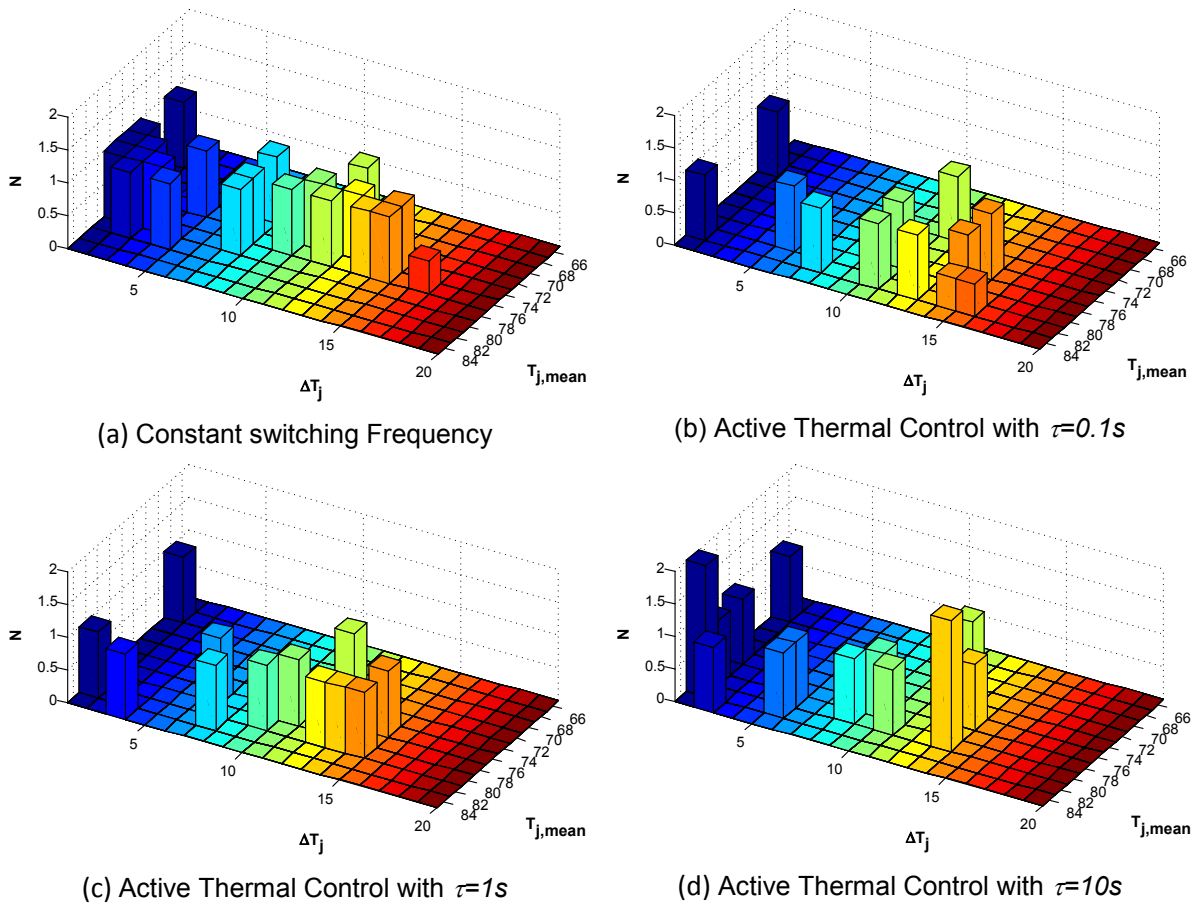

(a) Constant switching Frequency

(b) Active Thermal Control with τ=0.1s

(c) Active Thermal Control with τ=1s

(d) Active Thermal Control with τ=10s

Figure 6. Measurement results after rainflow counting for Diode D1.

	No thermal control	Thermal control, $\tau = 0.1s$	Thermal control, $\tau = 1s$	Thermal control, $\tau = 10s$
$T_{j,av}$ [°C]	75,85	81,76	80,54	80,71
$\sum \Delta T$ [K]	163,58	123,88	121,7	100,75
$f_{sw,av}$ [kHz]	10	14,60	15,02	14,90
$E_{loss,rel}$ [%]	100	107,4	105,7	106

Table 2. Comparison of the thermal stress in diode 1 for different controller settings.

It is inferred, that singular parameters as shown in table 1 and 2 cannot substitute the rainflow diagrams in the thermal stress analysis, because the loss of information related to the maximum thermal swing is important for the failure analysis. Additionally, it has to be considered that the application of a thermal management system can result in different failure mechanisms. An example for this could be that bond wire liftoff because of fast junction temperature fluctuation is less relevant and solder fatigue is getting dominant.

4) Conclusions

This work has presented an active thermal controller, with reduces thermal stress for power semiconductors during operation. The method does not require additional sensors and reduces thermal cycling by increase of the switching frequency when the output power is decreasing. With increased output power or after a specific time, which is dependent on the controller tuning, the semiconductor losses are minimized. Measurements show that the tuning of the controller is essential to reduce significantly the thermal swing and keep under control the increase of losses. Thermal cycles are reduced in magnitude and number by approximately 30% for all power semiconductors with the right tuning.

5) References

[1] Huai Wang; Liserre M., Blaabjerg F., "Toward Reliable Power Electronics: Challenges, Design Tools, and Opportunities", IEEE Industrial Electronics Magazine, vol.7, no.2, pp.17,26, June 2013.
[2] Smet V., "Aging and failure modes of IGBT power modules undergoing power cycling in high temperature environments", Ph.D. dissertation at Dept. Elect. Eng., Montpellier 2 University, November 2010.
[3] Hui H., Mawby P.A., "A Lifetime Estimation Technique for Voltage Source Inverters", IEEE Transactions on Power Electronics, vol. 28, pp. 4113-4118, Aug. 2013.
[4] Andresen, Markus, Marco Liserre, and Giampaolo Buticchi. "Review of active thermal and lifetime control techniques for power electronic modules." Power Electronics and Applications (EPE'14-ECCE Europe), 2014 16th European Conference on. IEEE, 2014.
[5] Murdock, Dustin A., et al. "Active thermal control of power electronic modules." Industry Applications, IEEE Transactions on 42.2 (2006): 552-558.
[6] Bayerer R., Herrmann T., Licht T., Lutz J., Feller M., "Model for Power Cycling lifetime of IGBT Modules - various factors influencing lifetime", 5th International Conference Integrated Power Systems (CIPS), 2008 March 2008.
[7] Wintrich A., Nicolai U., Tursky W., Reimann T., "Application Manual Power Semiconductors", SEMIKRON International GmbH.